Haptic Feedback to Assist Bus Drivers for Pedestrian Safety at Low Speed

Vicent Girbés, Leopoldo Armesto, Juan Dols and Josep Tornero

***Abstract*—Buses and coaches are massive Passenger Transportation Systems (PTS), because they represent more than half of land PTS in the European Union. Despite of that, bus accident figures are lower than other means of transport, but its size and weight increase the severity of accidents in which buses are involved, even at low speed. In urban scenarios, turnings and manoeuvres around bus stops are the main causes of accidents, mostly due to low visibility, blind spots or driver's distractions. Therefore, there is an increasing interest in developing driving assistance systems to avoid these situations, among others. However, even though there are some solutions on the market, they are not meant to work in urban areas at low speed and with the sole purpose of preventing collisions with pedestrians. In this sense, the paper proposes an active safety system for buses in manoeuvres at low speed. The safety system consists of haptic feedback devices together with collision avoidance and risk evaluation systems based on detected people nearby the bus. The performance of the active safety system has been validated in a simulated urban scenario. Our results show that driver's reaction time is reduced and time to collision increased due to the proposed low-speed active safety system. In particular, it is shown that there is a reduction in the number of high risk cases and collisions, which implies a considerable improvement in safety terms. In addition to this, a brief discussion about current regulations for innovative safety systems on a real vehicles is carried out.**

***Keywords*—Driver Assistance, Pedestrian Safety, Active Safety, Haptic Feedback, Emergency Braking, Collision Avoidance.**

I. Introduction

Buses and coaches are massive Passenger Transportation Systems (PTS) and they represent more than 50% of land PTS in the European Union (EU) [1]. Hence, there is a huge amount of people travelling and moving by this kind of vehicles every day. However, bus accident figures in Europe are on average significantly lower than in other means of transport (around 3% in 2004-2013 [2]), reaching the safety level of railway, metro and tram, despite the fact that bus and coach fleets share infrastructures with other users and transportation systems.

Nevertheless, in urban areas, the large flow of people using buses and walking around them implies a risk of accident, both as occupants and as pedestrians. As an example, in 2013 in the EU about 50% of fatalities in bus or coach accidents occurred in urban areas [2]. Moreover, in [3] it is claimed that almost 30% of those who died in 2013 in road accidents that involved buses or coaches were pedestrians.

For instance, in the USA from 2003 to 2012, 119 school-age children died in school-transportation-related crashes while they were moving around the vehicle [4]. Moreover, most accidents (crashes and fatalities) happened due to impacts in the front and right side of the bus. In fact, lack of visibility and distractions are by far the most common causes of bus accidents [2]. In most cases, the use of mirrors is insufficient because the location of a pedestrian may change quickly and/or the driver may be distracted. Therefore, even though governments and researchers have done a big effort in searching for solutions to improve active and passive safety systems for buses, there is still an urgent need to reduce the amount of fatalities and injuries all around the world.

Among the most used active safety systems in passenger buses for executing emergency braking, basically two must be mentioned: brake assistance system (BAS) and adaptive brake assist system (ABA). On the one hand, the BAS consists of a device that acts during emergency braking of the vehicle if the driver does not reach sufficient braking force to stop the vehicle in the shortest possible distance. If the force exerted on the brake pedal is not enough in an emergency situation, the BAS activates the brake booster or the electronic braking system (EBS) hydraulic unit increasing the total force exerted. The BAS interacts with: brake booster vacuum pump, anti-lock braking system (ABS), electronic stability program (ESP) and cruise control (ACC).

On the other hand, the ABA system detects a risk of rear-end collision against a vehicle in front of the bus at a lower speed or a stationary obstacle. The system reacts in stages with different types of visual, acoustic or brake assistance actions. The ABA system operates in motorways with three radar sensors that detect the presence of such vehicles on the front of the bus at a slower rate, so that it can automatically reduce the speed to restore and maintain the safety distance. Deceleration is limited to 20% of the maximum braking effort of the vehicle. Normally the radar sensors used are installed in the front of the vehicle and can detect obstacles up to a distance of 200 meters. In the last generation versions of this system, the operating speed range has been extended from 7 to 200 km/h [5].

In any traffic accident the critical pre-crash event or reason leading up to a crash can be assigned to any of the three factors involved: driver, vehicle or environment. However, the fact that between 70% and 90% among all traffic accidents are produced by a human factor is supported by some recent road safety reports from international institutions, such as the World Health Organization (WHO), the European Union Road Federation (ERF), or the National Highway Traffic Safety Administration (NHTSA) from the USA. For instance, in [6] it was explained that in the USA a driver error was involved in $94\% \pm 2.2\%$ of crashes. Among critical reasons attributed to drivers, recognition errors ($41\% \pm 2.2\%$) and decision errors ($33\% \pm 3.7\%$) were the most significant. These causes are closely related to distractions or slow response times, which are one of the main causes of accidents.

V. Girbés, L. Armesto, J. Dols and J. Tornero are with Instituto de Diseño y Fabricación at Universitat Politècnica de València, Spain

The authors of [7] analysed the psycho-motor reaction time (reaction time on the brake pedal) in a risky situation and showed that it varies in the range 0.42–0.92 s. As stated in [8], a study using both a real driving environment and a simulator showed that the reaction time of drivers to an anticipated danger in a real environment has a mean value of 0.42 ± 0.14 s whereas the mean value of the reaction time distribution to an unanticipated danger by extreme braking is about 1.1 s, being around 0.9 s in a simulator [9]. In the study carried out in [10] the authors proved that in real traffic situations the mean reaction time of drivers for unexpected and expected stimuli are also different, 1.3 s and 0.7 s respectively.

It is clear that anticipation of future traffic events provides potential gains in recognition and reaction times [11]. However, anticipation is not always possible in an urban environment in which pedestrians are involved, as their movements are sometimes fast and unpredictable. Moreover, there might be some manoeuvres in which the driver has low visibility, which make impossible any kind of anticipation. In this sense, the best approach to avoid accidents with pedestrians seems to be the detection of potential collisions and warning the driver to improve the reaction time. Thus the unexpected becomes expected and driver's reaction time improves.

During the last two decades researchers have developed many systems based on range sensor technologies, such as LIDAR, RADAR, ultrasound, cameras, among others; which are able to detect pedestrians or objects near the vehicle and to warn the driver in certain situations [12]–[16]. Once obstacles have been detected in the surroundings of the vehicle, haptic and audiovisual (HAV) warnings are produced to make the driver aware of the danger [17]–[20].

Particularly, the authors of [21] studied and proved the effectiveness of tactile and auditory pedestrian collision warnings in urban roads. [22] stated the growing interest among researchers in integrating haptic feedback into audiovisual systems, as haptics enhances the benefits of audiovisual feedback. In [23] human-machine cooperation when driving with different degrees of a shared control system was investigated. The authors of [24] evaluated the value of haptic feedback in the steering wheel for lane keeping. On the other hand, in [25] a haptic gas pedal for active car-following support was designed. See [26] for a detailed survey on the effect of haptic support systems on driver performance.

Therefore, by interacting with drivers and/or braking the vehicle all these safety systems try to modify their behaviour through reactive stimuli, with the aim of reducing the number of accidents and their severity. However, although there are some approaches and commercial solutions to avoid crashes between cars and pedestrians, their use in PTS is still in development and requires further research.

In this sense, the paper proposes the development and evaluation of a new active safety system with haptic feedback and emergency braking, to assist bus drivers in low-speed manoeuvres in urban scenarios (particularly in low visibility turnings and areas of passenger loading and unloading). That is covered in Sections II and III. Moreover, in Section IV the effectiveness of the developed safety system has been proven through some experiments carried out using a driving simulation cabin. Finally, some conclusions are drawn in Section VI.

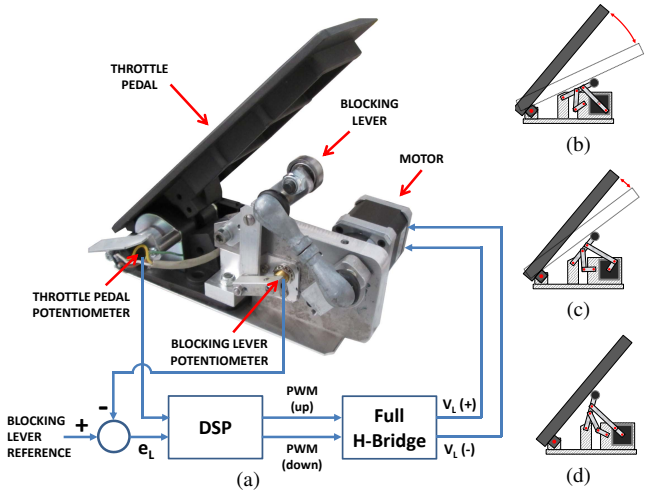

Figure 1. Haptic feedback system: (a) Haptic throttle with blocking lever, (b) Lower position, (c) Intermediate position, (d) Upper position.

II. Description of Safety Devices

In order to guide the driver or inhibit certain actions, our approach includes two kinaesthetic haptic feedback devices, one in the throttle pedal and another in the steering wheel. The system also incorporates an emergency brake system to avoid imminent collisions.

A. Haptic pedal

A motorized four-bar mechanism with a lever is placed in the throttle to *block* and eject the pedal in warning situations, as shown in Figure 1(a), while Figures 1(b), 1(c) and 1(d) show the lower, intermediate and upper positions respectively. Although only one intermediate position is shown, there are 11 configurations in between the lower and upper positions of the throttle.

It is worth mentioning that, here, the term *block* refers to capability to generate a torque opposite to driver's intention, to produce a kinaesthetic reaction and at the same time let the driver have complete control of the vehicle. These aspects are inferred from our experimentation in Section IV, as it will be explained thereinafter. In this sense, the haptic throttle has not been designed to ensure the absence of collisions, but as a warning system. When the lever tries to expel one's foot, one feels a force which is reasonably enough to warn, but at the same time, one can always push it back on purpose easily if needed.

For the throttle positioning, we use the closed loop control scheme shown in Figure 1(a). Either a full H-bridge or two half H-bridges drivers can be used to adapt the 2 PWM output signals from a DSP to control a 24V DC motor (each PWM for each motor direction). To be specific we used the high current H-bridge Infineon BTS 7960 chip and the 24V gear motor Büehler 1.61.046.333. In this sense, a proportional controller has been designed, where the gain K_L defines how aggressive the controller is, the lever reference r_L is set taking into account the level of risk of the manoeuvre, as will be explained

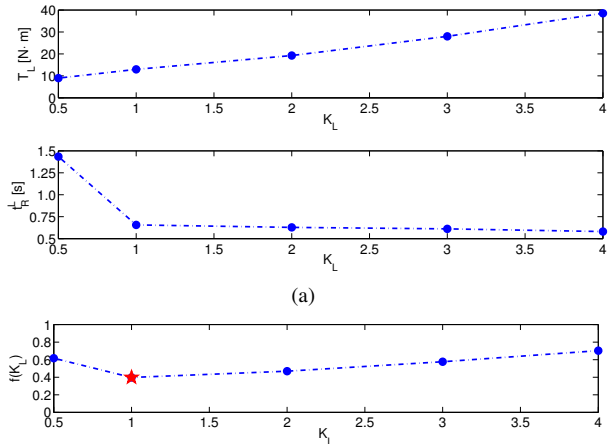

Figure 2. Throttle calibration. (a) Torque T_L and reaction time t_R for different values of K_L. (b) Cost function $f(K_L)$ with $a_L = 0.5$ and $b_L = 0.5$. Optimum value for gain $K_L^\star$ is the red star.

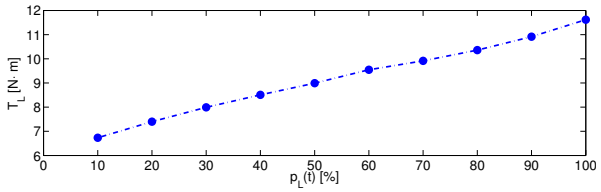

Figure 3. Throttle torque profile.

in Section III-C, the lever measured position is p_L and, by definition, the error variable is $e_L = r_L - p_L$:

$$PWM(up) = \begin{cases} K_L \cdot e_L & \text{if } e_L > 0, \\ 0 & \text{otherwise} \end{cases} \quad (1)$$

$$PWM(down) = \begin{cases} K_L \cdot e_L & \text{if } e_L < 0, \\ 0 & \text{otherwise} \end{cases} \quad (2)$$

The lever reference r_L is discretized into 11 positions, from 0% to 100% with increments of 10%. When the blocking lever position p_L is in the lower configuration ($p_L = 0\%$) the driver can freely push the throttle pedal to its maximum position (with an experimentally measured torque of 4.73 N$\cdot$m due to the original pedals spring (Electronic Heavy Duty Throttle Pedal 962 000 series, from Mobile Control Systems)).

An initial set of experimental tests has been performed in order to define the optimal torque values for the throttle haptic feedback device. In those tests, we adjusted different gains K_L so that we could select the value that optimizes a *comfort and safety* cost function. In this sense, we associate comfort to low values of the torque necessary to overcome the blocking and safety to the reaction time of the driver after the blocking device was enabled (the quicker response the higher safety). In particular, we measured the minimum torque to overcome the blocking lever torque ($T_L(K_L)$) in its upper position and the driver's time of reaction ($t_R^L(K_L)$) [1] for a given gain. Let $K_L^\star$ be the optimal gain of a performance function from weighted

[1]Defined as the time elapsed between the instant when the blocking lever is expelled and the time in which the driver releases the throttle and significantly presses the brake pedal.

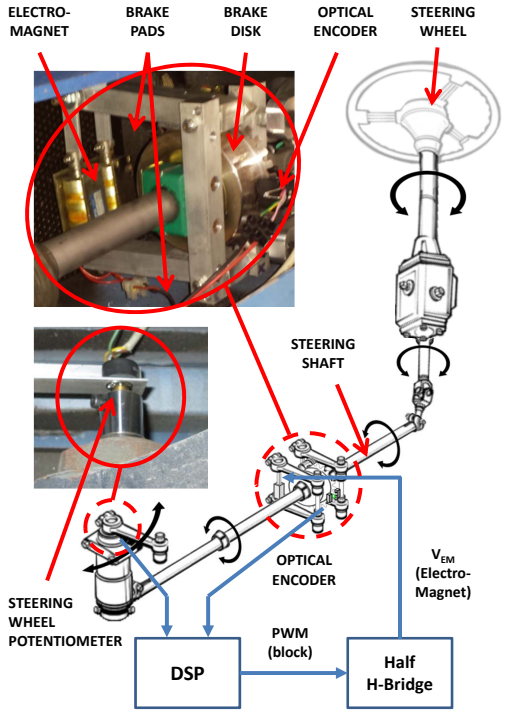

Figure 4. Steering column with active blocking system.

combination of both normalized variables T_L and t_R^L in the range 0 to 1:

$$K_L^\star = \underset{K_L \in [0,\infty[}{\operatorname{argmin}} f(K_L) = \underset{K_L \in [0,\infty[}{\operatorname{argmin}} \mathbb{E}\left[a_L \cdot T_L(K_L) + b_L \cdot t_R^L(K_L)\right] \quad (3)$$

where a_L and b_L are weights for each component and $\mathbb{E}$ is the expectation operator.

Figure 2(a) shows the profiles of T_L and t_R^L for different values of the controller gain K_L and Figure 2(b) shows the cost function with $a_L = 0.5$ and $b_L = 0.5$. For this particular weights selection, the optimal gain is $K_L^\star = 1$ and, as a result, when the lever is in the upper position ($p_L = 100\%$) the driver must apply a torque greater than 11.62 N$\cdot$m to move the *blocking* mechanism of the throttle. Another interesting aspect to show is the quasi-*linear* ratio between the lever position and the necessary torque for the selected gain, as shown in Figure 3. Note that there is no measure for $p_L = 0\%$, because in this case the haptic feedback is not enabled and therefore the lever is not blocking. In this situation the torque necessary to press the throttle pedal is the default value $T_T = 4.73$ N$\cdot$m, which depends on throttle model and manufacturer.

B. Haptic steering wheel

A kinaesthetic steering wheel has been implemented to cover situations where the haptic feedback in the pedal, mostly when the vehicle is turning, might not be necessary to press. This haptic device has been designed to be coupled in the steering wheel shaft in order to make the driver conscious of the side where the pedestrian comes from. In this sense, a braking system is placed in the steering column, which is composed by a brake disk and brake pads activated by an electromagnet

(a spring retracts the brake pads when the electromagnet is disabled), as shown in Figure 4. In order to accurately know driver's intention and reaction, an optical encoder is also included, together with the potentiometer that measures the steering wheel angle.

The system must allow normal driving when there is no collision risk, but making the driver aware if a potential collision is detected by *blocking* the steering wheel in the direction of a detected risk. Again here, the term *blocking* refers to introducing a momentary additional friction force on the steering wheel to produce the corresponding kinaesthetic reaction. In this way, the driver can perceive a constant resistance when moving the steering wheel towards the risky direction. The blocking force disappears as soon as the driver turns the steering wheel towards the opposite side or the risk vanishes.

A PWM signal regulates the electro-magnet voltage in the range $[0-24]$ V, which means that the brake friction can be also regulated using a half H-bridge (L293B from SGS-THOMSON). Following a similar procedure as in the throttle feedback design, we set different values of the voltage applied to the electromagnet (V_{EM}) and measured the minimum torque to overcome the blocking torque in the steering wheel (T_S). We also measured the driver's time of reaction ($t_R^S(V_{EM})$), understood as the delay between the instant when the blocking steering starts working and the time in which the driver changes the sense of turning towards the non-blocking side. Figure 5(a) shows the profiles of $T_S(V_{EM})$ and $t_R^S(V_{EM})$ for different values of the electromagnet input voltage V_{EM}.

To get the optimal value of V_{EM}, we normalize the variables T_S and t_S^L in the range 0 to 1 and define a cost function as a weighted combination of both components:

$$\begin{aligned} V_{EM}^{\star} &= \underset{V_{EM}\in[0,24]}{\operatorname{argmin}}\ f(V_{EM}) \\ &= \underset{V_{EM}\in[0,24]}{\operatorname{argmin}}\ \mathbb{E}\Big[a_S\cdot T_S(V_{EM})+b_S\cdot t_R^S(V_{EM})\Big] \end{aligned} \tag{4}$$

where a_S and b_S are the weights of each variable. Figure 5(a) shows the measured values and Figure 5(b) the cost function with $a_S=0.5$ and $b_S=0.5$. It can be seen that in this particular case, for the selected weights, the optimum is $V_{EM}^{\star}=24$ V, which suggests an ON/OFF control policy. As a result, the driver must apply a torque bigger than 4.34 N$\cdot$m when the haptic device is ON, which corresponds to the torque necessary to move the steering wheel and overcome the maximum dry friction of the electro-magnet used as blocking device.

C. Emergency Brake

It must be remarked that while emergency braking assistance systems such as BAS or ABA are designed to act when the bus travels at moderate speeds (over 60 km/h), the emergency braking system developed in this research has been designed to operate in passenger vehicles at low speed. Indeed, it has a threshold operation speed of up to 10 km/h, with a safety zone distance in front of the bus of about 5 m. This justifies the novelty of the research itself, since, to the authors' knowledge, in the current market it does not exist any ADAS developed

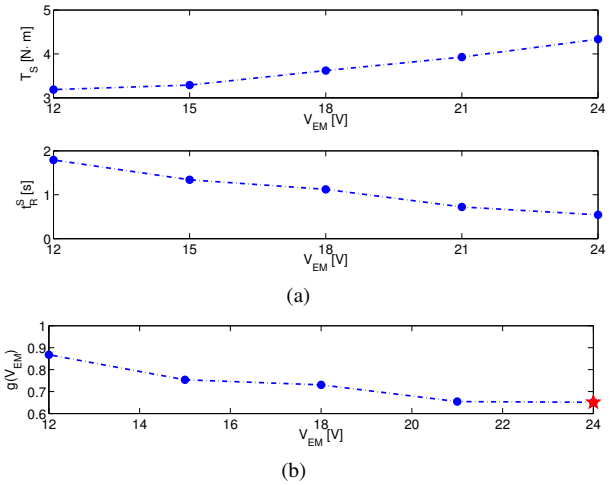

Figure 5. Steering calibration. (a) Torque T_S and reaction time t_R for different values of V_{EM}. (b) Cost function $g(V_{EM})$ with $a_S = 0.5$ and $b_S = 0.5$. Optimum voltage value is the red star.

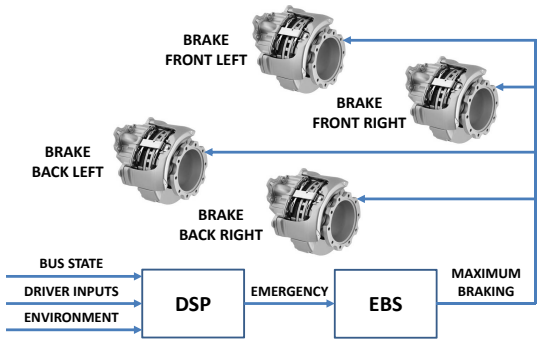

Figure 6. Emergency brake system.

for passenger vehicles in urban areas for buses, with the sole purpose of preventing collisions with pedestrians.

Our implementation on a real bus in [27] was achieved based on the diagram of Figure 6. In order to produce an automatic braking in risky situations, it is necessary to send an electronic signal to vehicle's braking system. However, the validation performed in Section IV uses a virtual environment and the braking system is simulated by applying a maximum brake after receiving such signal.

III. Methodology

A. Vehicle dynamics

In autonomous driving vehicles, obstacle avoidance algorithms are used to give specific speed commands to avoid collisions [28, Chapters 5 and 35]. They typically consider vehicle's state, nearby obstacles (obtained either from sensor readings or from a map) and a given target goal. In that sense, to allow the integration of generic obstacle avoidance frameworks into the driving assistance problem, existing algorithms must be adapted to provide valid solutions according to driver's intention.

In order to predict a potential collision, the system analyses not only vehicle's behaviour but also considers pedestrians moving around it. For that purpose, it is necessary to know

driver's intention, which is reduced to know the position of throttle, brake and steering wheel. It is interesting to remark that the following vehicle's dynamic model uses simplifications in order to achieve better computational performance in obstacle avoidance algorithms. This is a common approach in Robotics, where all unmodelled errors are reduced using safety margins [28, Chapters 5 and 35].

For simplicity, we assume that the vehicle moves in an $\Re^2$ workspace $\mathcal{W}$. So, its configuration space $\mathcal{CS}$ in $\Re^2 \times \mathcal{S}^1$ is $\mathbf{q}(t) = [x(t), y(t), \theta(t)]$, which indicates the Cartesian position and orientation of the vehicle, respectively. In addition to this, we define $\mathbf{u}(t) = [u_a(t), u_b(t), \alpha(t)]$ as the input vector containing the throttle pedal position $u_a(t)$, the brake pedal position $u_b(t)$ and the steering wheel angle $\alpha(t) \in [-\alpha_{max}, \alpha_{max}]$ with α_{max} as the maximum turning angle. We also assume that pedal ranges are normalized as follows: $u_a(t) \in [0, 1]$ and $u_b(t) \in [0, 1]$.

Following the ideas of [29], the non-linear longitudinal dynamics of a vehicle can be experimentally validated based on physical laws. Our validation data have been generated from a simulator using NVidia PhysX SDK 3.3.1, which comprises the complexity of the non-linear vehicle's dynamics. Settings of the simulation are given in Section IV based on real vehicle data.

Thus, based on [29], the components of vehicle's velocity $v(t) \in [0, v_{max}]$, with v_{max} as the maximum linear velocity, can be decomposed into two velocities:

$$v(t) = v_a(t) + v_b(t) \tag{5}$$

where $v_a(t)$ is related to acceleration and $v_b(t)$ to braking.

Due to the fact that the system is targeted to low-speeds, the non-linear effects of the longitudinal vehicle's dynamics can be neglected, in order to simplify computations. In this sense, the non-linear model for the acceleration component is approximated to a linearised first-order system as follows:

$$\frac{v_a(s)}{u_a(s)} = \frac{K}{\tau s + 1}, \frac{d(s)}{v_a(s)} = \frac{1}{s} \tag{6}$$

where $d(s) \equiv \mathcal{L}[d(t)]$ is the travelled distance, $v_a(s) \equiv \mathcal{L}[v_a(t)]$ and $u_a(s) \equiv \mathcal{L}[u_a(t)]$, being $\mathcal{L}$ the Laplace transform. Therefore, we assume that the vehicle follows an exponential expression and reaches a steady-state linear velocity $v_{ss}(t)$ by applying a constant input $u_a(t)$. Taking into account that τ is the time constant of the system, the time to reach such steady-state can be established as $t_{ss} \approx 5\tau$.

As shown in Figure 7, model identification has been done using a random input pattern, which provides a fitting performance of 96.57% for $K = 16.76$ and $\tau = 12.5$. This result has been also validated with a step response input pattern, which provided a fitting of 91.89%.

On the other hand, the model relating the effective deceleration can be expressed as an integrator:

$$\frac{v_b(s)}{a_b(s)} = \frac{1}{s} \tag{7}$$

with $v_b(s) \equiv \mathcal{L}[v_b(t)]$ the brake velocity component and $a_b(s) \equiv \mathcal{L}[a_b(t)]$ the brake acceleration component. The braking system of the simulated vehicle model depends on several

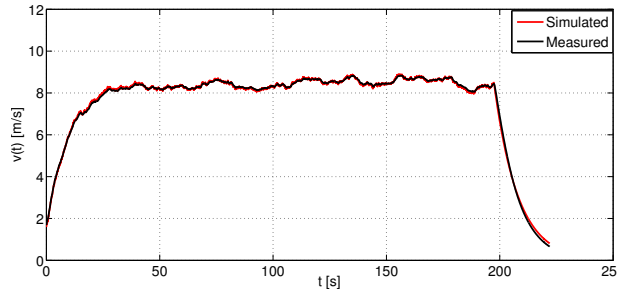

(a) Random input

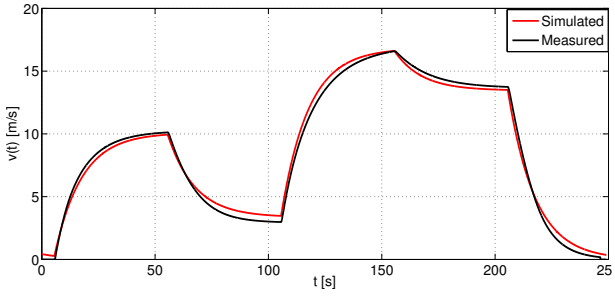

(b) Step input

Figure 7. Vehicle's dynamic model: (a) identification and (b) validation.

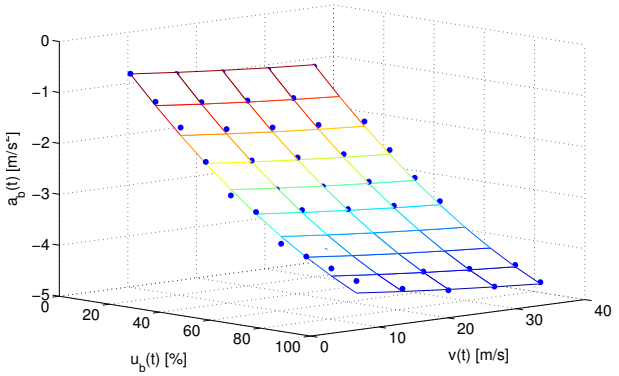

Figure 8. Deceleration surface. Blue dots are the values of $a_b(t)$ measured during the braking calibration tests.

variables, though the one that showed a higher influence is clearly the brake pedal position $u_b(t)$. It is also interesting to remark that there is some dependency on vehicle's velocity $v(t)$, although smaller, as shown in Figure 8. Based on these results, a two-dimensional second order polynomial braking model fitted with LS method (see Figure 8) is approximated:

$$a_b(t) \approx k_1 v(t) + k_2 v^2(t) + k_3 u_b(t) + k_4 u_b^2(t) \tag{8}$$

being $k_1 = -0.031$, $k_2 = 4.406 \cdot 10^{-4}$, $k_3 = -5.968$ and $k_4 = 1.792$ are the identified parameters. Notice that ideally vehicle's speed $v(t)$ should not affect the brake acceleration $a_b(t)$, but it does due to unmodelled non-linearities of vehicle, tires and road surfaces. However this effect is less significant than the brake pedal position $u_b(t)$, according to previous weights in (8).

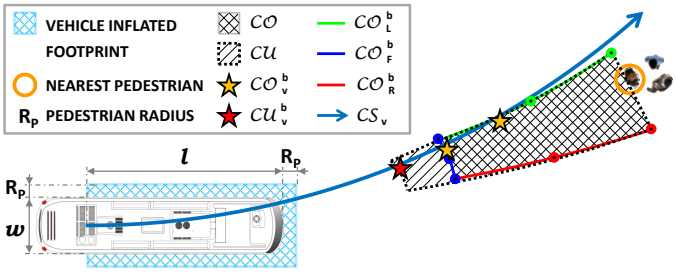

Figure 9. Example of collision detection.

B. Collision Detection

Now, let's define the two-dimensional manifold in $\Re^2 \times \mathcal{S}^1$ as the driver's configuration space $\mathcal{CS}_v$, obtained from a non-holonomic standard car-like kinematic model (*i.e.* type (1,1) in [28, Chapters 34 and 35]), describing arc segments from driver's commands (linear and angular velocities). Without loss of generality, $\mathcal{CS}_v$ has its center at (x_v, y_v) with $x_v = 0$, $y_v = \text{sign}(\alpha(t)) \cdot R_v(t)$ and radius $R_v(t) = \left|\frac{L}{\sin(\alpha(t))}\right|$, being $\alpha(t)$ the vehicle's steering wheel angle and L the wheelbase, *i.e.* distance between front and rear axles of the vehicle.

Based on Minkowsky addition [30], we can abstract the rectangular shape of the bus by enlarging the circle circumscribing a pedestrian to obtain an obstacle configuration space ($\mathcal{CO}$), as in Figure 9. This $\mathcal{CO}$ defines the region at which the vehicle collides with objects by describing an arc allowing to treat the vehicle as a point for further computations. Indeed, the configuration obstacle for all pedestrians is $\mathcal{CO} = \cup_i \mathcal{CO}_i$, where $\mathcal{CO}_i$ denotes the configuration obstacle for the i-th pedestrian. However, from now on, we neglect sub-index i to keep notation clearer, as if we were restricting the problem to one single pedestrian case, although computations are carried out, indeed, for every pedestrian. Let's denote $\{x^b_{\mathcal{CO}}, y^b_{\mathcal{CO}}\} \in \mathcal{CO}^b$ the boundary points for a given pedestrian position $\{x_p, y_p\}$, being $\mathcal{CO}^b$ the boundary of $\mathcal{CO}$.

However, instead of considering the whole analytic $\mathcal{CO}^b$, in our approach we only consider mid and end points of each segment of the rectangular shape. This reduces the computation of shape abstraction to a total of 7 points (dots in Figure 9). Furthermore, we approximate $\mathcal{CO}^b$ with 3 arc segments, one for every triple of points related with each segment of the rectangle:

$$\mathcal{CO}^b \approx \mathcal{CO}^b_L \cup \mathcal{CO}^b_F \cup \mathcal{CO}^b_R \tag{9}$$

where $\mathcal{CO}^b_L$ denotes configuration obstacle boundary for left-side, $\mathcal{CO}^b_F$ corresponds to the front-side and $\mathcal{CO}^b_R$ to the right-side. As a consequence, $\mathcal{CO}^b$ becomes a piece-wise function formed with 3 arc segments (green, blue and red lines in Figure 9).

Now, let's define $\mathcal{CO}^b_v = \mathcal{CO}^b \cap \mathcal{CS}_v$ as the manifold in $\Re^2 \times \mathcal{S}^1$ in which vehicle configurations are in collision with objects. This manifold is indeed computed from geometric relations between arc segments. For every segment of the vehicle shape, we compute the intersection between the arc segment defined by $\mathcal{CS}_v$ and the approximation of $\mathcal{CO}^b$ in (9). If such intersection point exists and belongs to both arc segments, it is considered as a candidate collision point. The point with the minimum distance (arc-length to reach that point from the origin) is the most critical one and, thus, the one to be considered. Such distance is denoted as $d_{\mathcal{CO}}(t)$ and computed as follows:

$$d_{\mathcal{CO}}(t) = \min_{i \in \mathcal{C}(t)} R_v(t)\delta_i(t) \tag{10}$$

being $\mathcal{C}(t)$ the subset of candidates collision points and $\delta_i(t)$ their arc angle.

There exists an unsafe obstacle configuration space ($\mathcal{CU}$), which defines the region for inevitably collisions due to vehicle's dynamics. Indeed, $\mathcal{CO} \subset \mathcal{CU}$, which contains additional vehicle's configurations that are unsafe, because of the needed distance to stop the vehicle in case of emergency braking. Computing $\mathcal{CU}$ for a general obstacle avoidance problem is complex as it requires to compute four additional boundary points for every boundary point of $\mathcal{CO}$.

Therefore, ADAS system must consider $\mathcal{CU}$ instead of $\mathcal{CO}$ to take decisions including vehicle's dynamics. $\mathcal{CU}^b_v = \mathcal{CU}^b \cap \mathcal{CS}$ is interesting because it considers driver's intention, being $\mathcal{CU}^b$ the boundary of $\mathcal{CU}$. The computation of the distance to collision along $\mathcal{CU}^b_v$ is as follows:

$$d_C(t) = d_{\mathcal{CO}}(t) - d_{min}(t) \tag{11}$$

with $d_{min}(t)$ a distance related to the distance necessary to stop the vehicle, which will be defined thereinafter.

In addition to this, we can also express such distance as follows:

$$d_C(t) = \int_t^{t+t_C} v(\tau) d\tau \tag{12}$$

where t_C is the time to collision, which will be used as measure of safety in Section IV.

C. Risk evaluation

Following the premise of most Adaptive Cruise Control (ACC) systems [31], in order to safely decelerate a vehicle to avoid a potential collision with the closest obstacle, the minimum stop distance $d_{stop}(t)$ is dynamically computed to guarantee that the vehicle can stop by applying the maximum braking deceleration $a_{b,max}(t)$:

$$d_{stop}(t) = 0.5 \cdot v(t)^2 / a_{b,max}(t) \tag{13}$$

where $a_{b,max}(t)$ is obtained for $u_b(t) = 1$ from the model identified in (8).

In order to introduce an additional safety factor, we define $d_{min}(t)$ as follows:

$$d_{min}(t) = d_{safety} + d_{stop}(t) \tag{14}$$

where d_{safety} is a safety distance where to *theoretically* stop the vehicle with respect to an object.

Furthermore, the maximum threshold distance for the collision risk factor is defined as:

$$d_{max}(t) = d_{min}(t) + \Delta d(t) \tag{15}$$

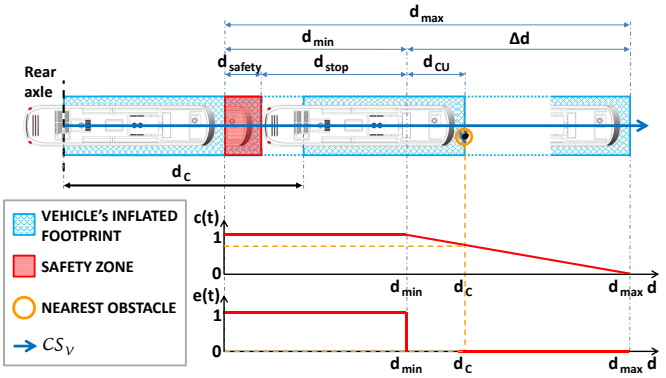

Figure 10. Example of frontal collision risk evaluation.

where $\Delta d(t)$ is a design parameter representing the anticipation distance in which the vehicle should reduce its speed before reaching the "inevitable collision" distance $d_{min}(t)$.

So, high values of $\Delta d(t)$ imply conservative solutions with anticipated warning, since the ADAS system becomes active sooner. On the contrary, low $\Delta d(t)$ values mean less conservative solutions with sharper transition from warning to emergency braking. As $\Delta d(t)$ is a design parameter, one can typically set it to a constant value or define an expression dependent on vehicle's velocity.

Figure 10 shows the definition of variables related to the risk factor for a frontal collision. The same concepts apply to any arbitrary $\mathcal{CS}_v$, where previously defined distances, $d_{min}(t)$ and $d_{max}(t)$, are indeed arc-lengths.

In order to assist the speed control of the vehicle, we propose the following collision risk factor to be evaluated:

$$c(t) = \text{sat}_{[0,1]}\left(\frac{d_{max}(t) - d_C(t)}{d_{max}(t) - d_{min}(t)}\right) \tag{16}$$

where $d_{min}(t)$ and $d_{max}(t)$ are distance thresholds that define a spatial window where the system is active: 1) if $c(t) = 0$ there is no risk of collision; 2) if $c(t) \in]0, 1[$ the system is not in collision, but there is a potential risk of collision and thus warning must be activated; 3) if $c(t) = 1$ there is a maximum risk of collision and therefore emergency braking must be applied.

On the one hand, the haptic feedback on the throttle is only useful when the driver is pressing it. For this reason, our ADAS system generates a warning signal $w(t)$ to control the position of the throttle blocking lever, being its angular position proportional to $w(t)$. The warning signal $w(t)$ is based on the risk factor $c(t)$ and it is conditioned to pressing the throttle:

$$w(t) = \begin{cases} c(t) & \text{if } u_a(t) > 0 \text{ and } v(t) > 0, \\ 0 & \text{otherwise} \end{cases} \tag{17}$$

On the other hand, if $c(t) = 1$, then emergency braking must be applied. In such cases, an emergency signal $e(t)$ is enabled in order to stop the vehicle conditioned to vehicle's velocity:

$$e(t) = \begin{cases} 1 & \text{if } c(t) = 1 \text{ and } 0 < v(t) < v_{e,max}, \\ 0 & \text{otherwise} \end{cases} \tag{18}$$

with $v_{e,max}$ a threshold speed to disable the emergency braking if vehicle's velocity is above this value as the people detection system may become unreliable. Besides, $v_{e,max}$ is used in order to comply regulations because emergency braking cannot be applied if speed is above certain values.

Figure 11. Driving simulation cabin with projection system composed by 3 projectors and a semicircular screen.

Regarding the feedback in the steering wheel, we propose the following steering risk factor:

$$s(t) = \begin{cases} s_v & \text{if } c(t) > 0 \text{ and } s_v = s_p \text{ and } \frac{|\kappa_v| - |\kappa_p|}{\kappa_{max}} < -\epsilon, \\ -s_v & \text{if } c(t) > 0 \text{ and } s_v = s_p \text{ and } \frac{|\kappa_v| - |\kappa_p|}{\kappa_{max}} > \epsilon, \\ 0 & \text{otherwise} \end{cases} \tag{19}$$

with $\kappa_{max} = \sin(\alpha_{max})/L$, $\kappa_v = \sin(\alpha(t))/L$ and $\kappa_p = 2\sin(\beta)/d_p$, the maximum and current curvatures of the vehicle, and the curvature of the circular arc joining vehicle and pedestrian, respectively; where $s_v = \text{sign}(\kappa_v)$ and $s_p = \text{sign}(\kappa_p)$ are the signs of these curvatures; being $d_p = \sqrt{x_p^2 + y_p^2}$ and $\beta = \arctan(y_p, x_p)$ the distance and angle to the pedestrian position, with x_p and y_p the pedestrian's coordinates with respect to vehicle's local reference system. ϵ is a design parameter that defines a dead zone of non-blocking for curvatures with similar values. For instance, usual values for ϵ are $0.05 - 0.1$. Note that taking into account the criterion in which positive curvatures imply turning to the left, we define $s(t) = 1$ for left blocking and $s(t) = -1$ for right blocking.

IV. Experimental Results

In order to evaluate the performance of the proposed safety system, several experiments were carried out using a driving simulator, as shown in Figure 11. The set of experiments for the benchmarking was conducted on 20 different drivers in an urban scenario (a small area of the city of Valencia). All drivers had driving licence and were between 20 and 55 years old. Although there were people from different ages and genders, these factors are not evaluated in this paper.

Two different tests were carried out to evaluate and compare certain aspects of the safety system, as will be explained next. For both experiments, the safety distance was set to $d_{safety} = 1$ m. The model of the simulated bus was dynamically adjusted to be equivalent to the real bus used in [27]. The traffic management, including traffic lights, artificial intelligence of cars and pedestrians were also developed to make simulation more realistic, as can be seen in Video #1 of Appendix A.

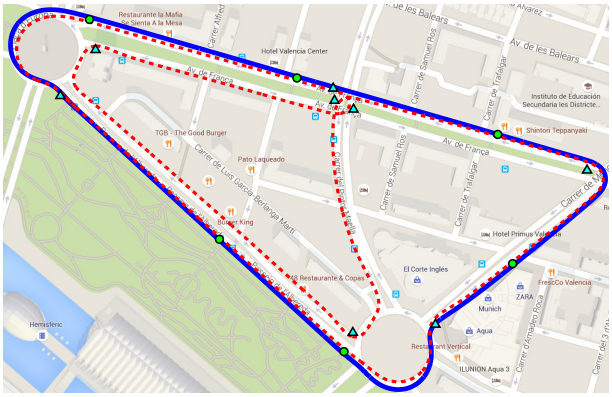

Figure 12. Urban scenario with two different bus routes. The first route (blue line) has 6 bus stops (green dots) and it is used to evaluate the performance of the haptic throttle and the emergency braking. The second bus route (red dashed line) has 8 turnings (cyan triangles) and allows the evaluation of the haptic feedback in the steering wheel in risky situations in corners.

The aim of such experiments is to evaluate the performance of the proposed safety system. Several aspects will be analysed in Sections IV-A and IV-B, such as percentages of low, medium, high risk incidents and collisions, as well as driver's reaction time in warning situations and time to collision in emergency situations. In the experimentation, we consider the following risk conditions:

- **Low**: when $d_{min} < d_C \leq d_{max}$.
- **Medium**: when $d_{safety} < d_C \leq d_{min}$.
- **High**: when $0.1\text{m} < d_C \leq d_{safety}$ and $v > 1.5$ m/s.
- **Collision**: when $d_C \leq 0.1\text{m}$ and $v > 0.6$ m/s.

Accordingly, the three proposed safety systems are expected to be effective upon the cases shown in Table I.

Table I. SAFETY SYSTEM EFFECTIVENESS

System	Low	Medium	High	Collision
Haptic throttle pedal	X	-	-	-
Haptic steering wheel	X	-	-	-
Emergency brake	-	X	X	X

As stated in Section I, drivers' reaction time t_R is approximately between 0.4 s and 0.9 s on average [7]. In our experimentation, the time of reaction was measured as the delay between the instant in which a pedestrian appears and the time instant when the driver presses the brake pedal, at least, a 10% of its range. Empirically, t_R varies from 0.3 s to 1.2 s. We discarded values of $t_R < 0.3$ s because either, the driver was already pressing the brake pedal or the driver's intention was to brake before the possible incident. In addition to this, we also measure the time to collision, as the time that the vehicle travels d_C (12). In both metrics, we want to obtain the worst case per driver, so the following formulas are applied:

$$m_C^{[i]} = \min \mathbf{t}_C^{[i]} \tag{20}$$

$$m_R^{[i]} = \max \mathbf{t}_R^{[i]} \tag{21}$$

where i denotes the i-th driver, being $\mathbf{t}_C^{[i]}$ and $\mathbf{t}_R^{[i]}$ the lists corresponding to metrics with all medium risk, high risk or collision incidents involving the i-th driver. It is interesting to remark that the time of reaction t_R is computed for all cases, whilst for the time to collision t_C only emergency situations are taken into account, which involve incidents of medium and high risk, plus collisions.

A. Haptic throttle and emergency braking

For this test, drivers were addressed to take 4 loops to the first route, stopping the vehicle on each of the 6 bus stops (blue line and green dots in Figure 12). In order to force unexpected dangerous situations around bus stops, pedestrians showed up randomly by walking in front of the bus, either when it was about to stop or when it was going to start its movement just after a bus stop. Video #2 of Appendix A shows an example of a subject using the driving simulator with the safety system active. It is worth mentioning that people participating on the test did not know when or where a pedestrian was going to appear and, furthermore, half the times the haptic throttle and the emergency braking were randomly disabled, so the driver did not know whether the system was active or inactive.

The test produced 606 incidents (half with the safety system OFF and half with it ON) classified as low risk (Low), medium risk (Med), high risk ($High$) and collision (Col), as shown in Table II. A proper discussion about these and other results from this set of tests will be carried out in Section V-A.

Table II. RISK EVALUATION OF TESTS WITH HAPTIC THROTTLE AND EMERGENCY BRAKING DISABLED (OFF) AND ENABLED (ON).

Haptic Feedback	RISKY INCIDENTS				
	Low	Medium	High	Collision	Total
OFF	179	83	39	2	303
ON	184	108	11	0	303

A total of 960 incidents could have happened during the tests, because there could be up to 2 incidents per bus stop (approach and departure), with 6 bus stops per loop, 4 loops per driver and 20 drivers. But, there were 606 incidents, which means 1.26 risky situations around each stop, on average. This happens because pedestrians appeared in a random pattern before or after a bus stop, in both cases or in none of them. However, as this happened randomly, drivers did not know when or where a pedestrian was going to show up. Perhaps, we could have reduced the number of incidents by doing them more "unusual". However, after analysing the average value of reaction time in the first 20 incidents occurred to any of the drivers, we found that there is no pattern in which the time of reaction is reduced, but random values around the mean value. So, it can be concluded that there is no "learning effect" and the time response is not altered.

We decided to analyse the metrics for each driver and not for the whole amount of incidents together, as some aspects could be diluted in the average value. Actually, in Figures 14, 15 and 17, the number should sum up to 80 (4 subfigures and 20 drivers), not all 606 incidents, because the population is at most 20 for each case, as there are 20 drivers. From Equations (20) and (21), the metrics for each driver can be computed. Then, the histogram and distribution of those cases in either situation (approach/departure and ON/OFF) is depicted. However, as can be noticed there are some histograms with less than 20 values, due to the fact that some people did not have incidents or were discarded either in approach or departure manoeuvres.

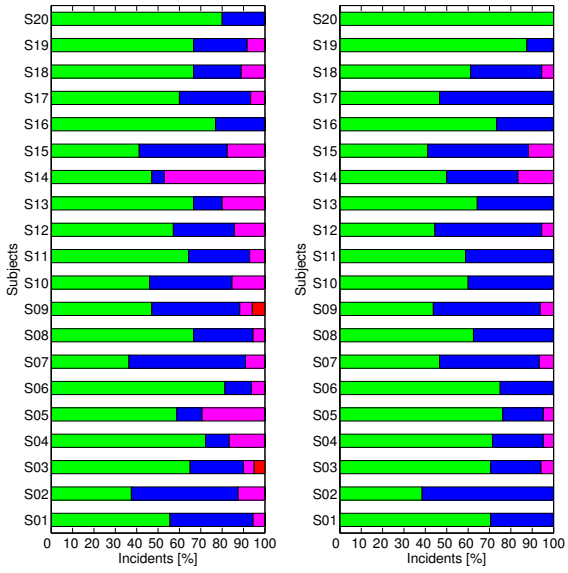

(a) OFF (b) ON

Figure 13. Bar diagram with incidents happened to each driver around bus stops, with haptic throttle and emergency braking (a) disabled and (b) enabled: (green) low risk, (blue) medium risk, (magenta) high risk and (red) collision.

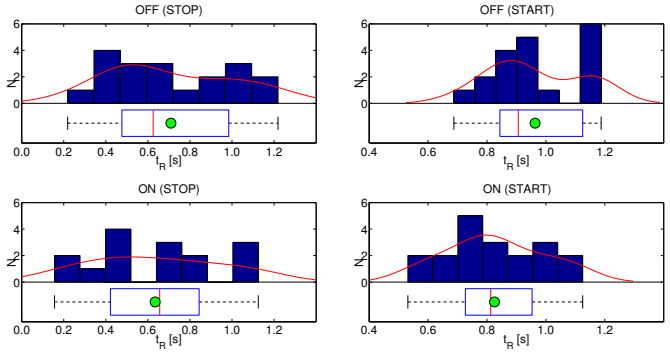

(a) Approach (b) Departure

Figure 14. Histograms and distributions of reaction time t_R, when ADAS is OFF (up) and ON (down): (a) t_R in approach manoeuvres (STOP) and (b) t_R in departure manoeuvres (START).

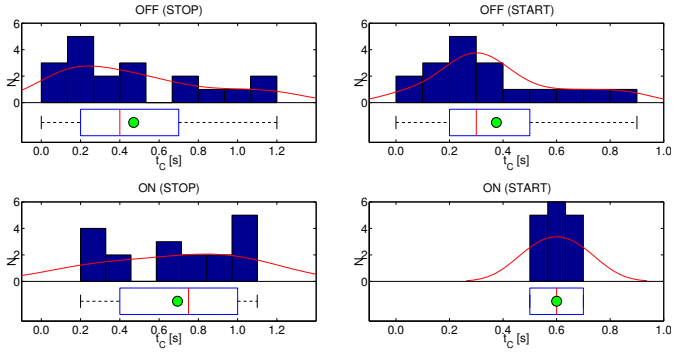

(a) Approach (b) Departure

Figure 15. Histograms and distributions of time to collision t_C in emergency situations, when ADAS is OFF (up) and ON (down): (a) t_C in approach manoeuvres (STOP) and (b) t_C in departure manoeuvres (START).

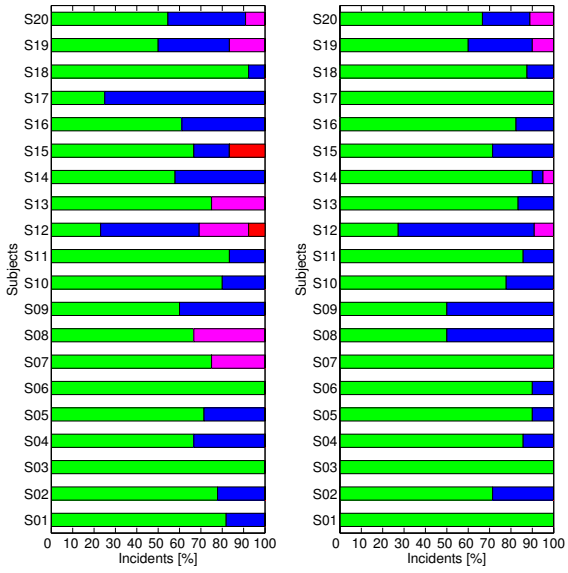

(a) OFF (b) ON

Figure 16. Bar diagram with incidents happened to each driver in turnings, with the steering feedback (a) disabled and (b) enabled: (green) low risk, (blue) medium risk, (magenta) high risk and (red) collision.

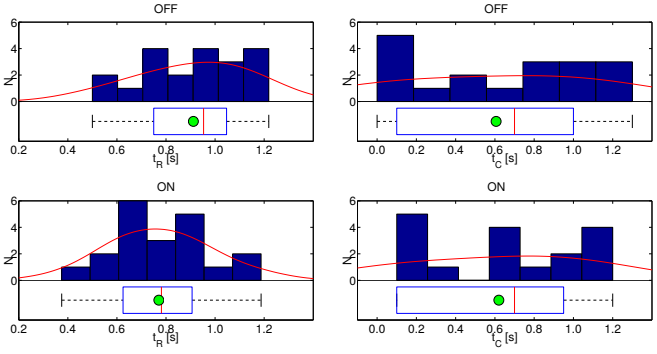

(a) Reaction time t_R (b) Collision time t_C

Figure 17. Histograms and distributions of t_R and t_C in turning incidents.

In Figure 13, a bar diagram with all incidents around bus stops of every driver is plotted. For each subject, the left graph is for cases with the haptic feedback and emergency braking disabled (OFF), while the right bar diagram is for incidents in which the haptic and emergency systems are enabled (ON).

Now, we focus on analysing separately situations where the vehicle is approaching the bus stop (STOP) and those in which it departs (START). In both cases, we compare the results when the safety haptic system is disabled (OFF) and when it is enabled (ON). Figure 14 shows the results considering the reaction time t_R, while in Figure 15 the results obtained for the time to collision t_C are depicted.

B. Haptic steering wheel

To evaluate the performance of the haptic feedback in the steering wheel, a different route is proposed which includes more turnings (red dashed line and cyan triangles in Figure 12). As in the first set of experiments, the subjects were addressed to drive normally around the city and to take 4 loops to a predefined circuit, but, in this case they did not have to stop.

On each turn, a pedestrian randomly appeared walking in front of the bus from either the left or the right side of the street. By doing this, subjects did not expect when and where pedestrians were going to show up from. In this experimentation, the throttle safety system was always enabled (haptic warning and emergency braking), but half the times the haptic feedback in the steering wheel was randomly disabled, in order to evaluate its performance and possible benefits.

As can be seen in Table III, the test produced an amount of 346 incidents, combining cases in which the haptic steering feedback was disabled with cases when it was enabled (we registered 173 incidents on each situation). When the feedback in the steering wheel was disabled there were 112 incidents considered as low risk, while 135 cases when it was enabled, reducing the number of medium risk, high risk and collision incidents. Figure 16 shows the results obtained per individual.

Table III. RISK EVALUATION OF TESTS PERFORMED WITH THE STEERING FEEDBACK DISABLED (OFF) AND ENABLED (ON).

Steering Feedback	RISKY INCIDENTS				
	Low	Medium	High	Collision	Total
OFF	112	48	9	4	173
ON	135	33	5	0	173

Finally, in Figure 17 the time to collision t_C and reaction time t_R of the drivers in turnings is shown. This will help to compare the performance when the haptic steering is disabled (OFF) and when it is enabled (ON). In Section V-B we discuss the results obtained and draw some conclusions.

C. Usability

In order to analyse the usability of the safety system from drivers' experience, after finishing the driving tests they were asked to complete a short questionnaire regarding their opinion about comfort and safety. They had different options to choose in a range from 1 to 5 to refer to the degree of agreement with the statement (higher the better). Table IV shows the results of the survey. Questions 1-3 are related to comfort, whilst questions 4-7 are about safety.

Table IV. RESULTS FROM USERS EXPERIENCE AFTER DRIVING TESTS.

Questions	Answers
Q1. The ADAS is not annoying in normal driving situations.	4.6
Q2. The blocking torque in the throttle pedal is correct.	3.9
Q3. The blocking torque in the steering wheel is correct.	4.1
Q4. The haptic warning in the throttle pedal is helpful.	4.5
Q5. The haptic warning in the steering wheel is helpful.	4.3
Q6. The haptic feedback works in low risk situations.	4.5
Q7. The emergency stop works in dangerous situations.	4.6

V. DISCUSSION

A. Haptic throttle and emergency braking

If we analyse Table II, when the system was disabled there were 179 situations considered as low risk incidents, 83 medium risk incidents, 39 high risk and 2 collisions. On the contrary, when the haptic throttle and the emergency braking were enabled, it can be clearly seen that a total of 30 previous cases, including high risk and collisions, were now considered as low or medium risk incidents. In our opinion, this can be mainly attributed to the emergency braking, which is able to stop the vehicle avoiding a crash when the driver does not react in time. Only 5 more cases have been now considered as low risk, which could be directly attributed to the haptic feedback.

As it can be clearly seen in Figure 13, the system improves reducing the number of high risk incidents and collisions to all drivers. In general, the number of these incidents are reduced although there are 5 cases in which the ratio increases (individuals 6, 11, 12, 17, 18). However, in those cases the ratio of low risk incidents is higher, which implies that the haptic system was effective despite of the high number of incidents.

Furthermore, if we analyse the average values for all drivers of the different risky incidents, we observe a considerable improvement. When the safety system is OFF, drivers on average tend to have 59.66% of low risk, 27.62% of medium risk and 12.18% of high risk incidents, with a 0.54% of probability of collision. On the contrary, when the system is ON a 62.13% of incidents are low risk, 34.48% are medium risk and 3.39% are high risk, without any probability of collision. Hence, it can be said that the force feedback in the throttle and the emergency braking help to reduce the number of high risk incidents and collisions. At the same time, the ratios of low risk and medium risk incidents are increased, which is an improvement in safety.

It can be observed in Figure 14(a) that the time of reaction is slightly better when the haptic throttle is enabled (mean value $t_R \approx 0.63$ s) than when it is disabled (mean value $t_R \approx 0.71$ s) when stopping the vehicle. In addition to this, when departing the haptic system becomes more effective with an improvement around 15% faster regarding the reaction time: mean value $t_R \approx 0.82$ s when ON against $t_R \approx 0.96$ s when OFF in mean, as shown in Figure 14(b). On the other hand, in Figure 15(a) it can be observed that the probability distribution function of the time to collision when approaching is a combination of two Gaussian distributions. On one side, there are people who react later and produce lower times to collision $t_C \approx 0.3$ s, on average. Whilst on the other, some drivers are more conservative and their mean time to collision is much higher $t_C \approx 0.9$ s. However, with the haptic throttle enabled the distribution function tends to move to the right (increases the number of time to collision cases with $t_C \geq 0.6$ s). Furthermore, as it is shown in Figure 15(b), the time to collision in departure situations is clearly improved, reducing considerably the standard deviation (SD) and moving the mean value from $t_C \approx 0.37$ s to $t_C \approx 0.6$ s (roughly twice and even bigger for the median).

In order to validate results, we have performed an analysis of variance (a two-way ANOVA) to evaluate if the differences observed are statistically significant considering the factors *haptic throttle* and *driver*. The purpose is to determine whether data from the levels of the factor *haptic throttle*, corresponding to OFF and ON, and levels of the factor *driver* corresponding to each subject, have a common mean or, on the contrary, are significantly different.

From ANOVA tests, we get that the *p*-value corresponding to the time to reaction t_R when the vehicle approaches the bus stop for the factor *haptic throttle* is $p = 0.124$ and for the factor *driver*, we get $p = 0.091$. This means that either null hypothesis

cannot be rejected at the 5% significance level. Therefore, we can conclude that the observed differences in the reaction time are not statistically significant. On the contrary, if we analyse the time of reaction in departure manoeuvres, after ANOVA analysis, we get that $p = 0.01$ for the factor *haptic throttle*. Therefore, we reject the null hypothesis and can conclude that both groups of data are statistically different with a significance of 5%. Hence, the haptic feedback in the throttle do influence the time of reaction in departure manoeuvres. On the other hand, the factor *driver* provides $p = 0.196$. So, we cannot reject the null hypothesis and prove that the two samples are not statistically different (5% of significance level) and hence the time of reaction is not influenced by the factor *driver*. This is also interesting because it means that the haptic feedback performance is similar for all type of drivers (let's say normal, conservative, aggressive).

Now, we consider the ANOVA analysis regarding the time to collision t_C in approaching manoeuvres involving the factor *emergency brake*, which takes its two possible levels OFF/ON and the factor *driver*. The factor *emergency brake* clearly provides a statistic significance of 5%, since $p=0.03$. Whilst the factor *driver* has not significance because $p = 0.132$. Therefore, we state that the observed improvements in t_C are due to the usage of the proposed emergency brake system with 5% of significance, but are not influenced by the driver. Regarding departure manoeuvres the results are very similar. From ANOVA we get that the factor *emergency brake* affects the time to collision because $p=0.006$. But, as $p=0.512$ for the factor *driver*, t_C does not vary significantly for different drivers.

B. Haptic steering wheel

Table III shows that when the haptic feedback in the steering wheel was enabled the number of medium risk, high risk and collision incidents was reduced. This means that the steering feedback improves safety, as this warning helps the driver react faster and avoids unnecessary emergency braking.

On the other hand, Figure 16 shows the results obtained per individual, where again there are situations in which the system tends to reduce the number of incidents. Now, if we analyse the average values for all drivers of the different risky incidents we observe an improvement. When the system is OFF, drivers tend to have 68.41% of low risk, 23.76% of medium risk and 6.61% of low risk incidents, with a 1.21% of probability of collision. On the contrary, when the system is ON a 78.46% of incidents are low risk, 19.78% are medium risk and 1.76% are low risk, with no collisions. So, the haptic feedback in the steering wheel tends to increase the percentage of low risk incidents while reducing the number of high risk and collision accidents.

Next, we analyse and compare the time of reaction t_R when the steering feedback was disabled and when it was enabled. As shown in Figure 17(a), in turnings when the steering feedback is OFF the average time of reaction was $t_R \approx 0.91$ s, which is 15% slower than when it is ON ($t_R \approx 0.77$ s). After analysing the ANOVA results we conclude that the differences for the factor *haptic steering* are statistically significant because $p=0.0196$. However, as in the previous set of experiments the factor *driver* is not significant since $p=0.09$. On the other hand, it is worth mentioning that we also have analysed the time to collision t_C (see Figure 17(b)), which provides no significance according to the ANOVA analysis. This makes perfect sense, since the haptic steering feedback is only effective at low risk situations as shown in Table I.

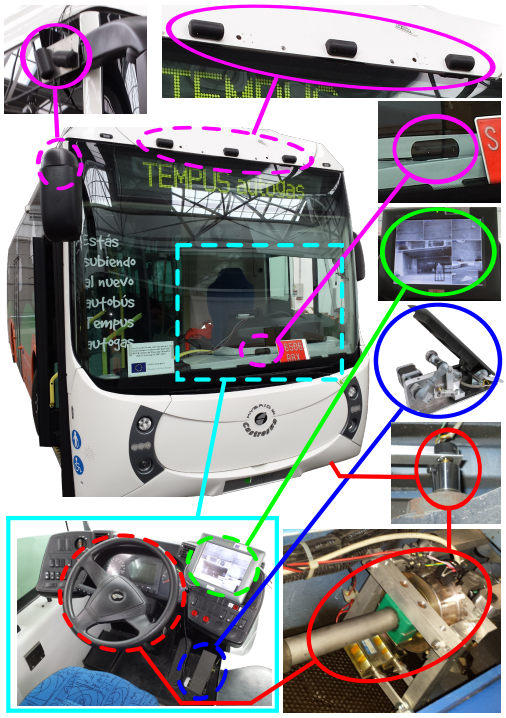

Figure 18. Implementation of the proposed safety system in a real bus: (magenta) network of smart cameras, (green) audio-visual feedback, (blue) haptic feedback in the throttle and (red) haptic feedback in the steering wheel.

C. Usability

In general the results shown in Table IV are good, as most items have a mark above 4 out of 5. Questions Q2 and Q3 are the lower ones, close to 4. The answers derived from these items might imply that people using the system felt some slight kind of discomfort, however this could be simply attributed to their lack of previous experience using the system.

D. Regulation

The implantation of the proposed active safety system into city buses seeks to reduce the frequency and severity of accidents related to buses. However, it is worth noting that the developments made in this paper are still in a prototype stage. So, their implementation in real systems is not immediate, requiring compliance with current legislation and relevant approvals. We believe that the haptic steering wheel feedback is compliant with the vehicle's steering equipment (Regulation UN/ECE 79), because the driver remains in primary control of the vehicle but may be helped by the steering system being influenced by signals initiated on-board vehicles of type M3 (buses). On the other hand, Regulation UN/ECE 13 applies for the vehicle's emergency braking system. The proposed system must be compliant with this regulation, which might imply the integration within the Electronic Braking System ECU.

Finally, regarding the haptic feedback in the throttle pedal, the system does not affect the original vehicle configuration. Besides, unlike for the brake there is no-regulation regarding the maximum force that can be applied to the throttle pedal, it only depends on the bus manufacturer. In any case the torque necessary to overcome the force of the lever is small enough to allow a normal driving.

All these regulation aspects have been taken into account during the development of our preliminary pedestrian detection and emergency brake system in the context of the SAFEBUS project, see [27] for further details. As a result of the project we were able to perform some preliminary tests using a real bus, as shown in Figure 18, which constituted a proof of concept for the proposed systems in this paper. The experimentation included exactly the same haptic feedback devices in throttle and steering wheel and emergency brake system. It also included a set of smart-cameras, placed in the periphery of the bus to detect pedestrians in vehicle's surroundings and audiovisual feedback through a standard monitor screen, which are out of the scope of this paper.

VI. Conclusions

The development of a new advanced outdoor safety system for buses in urban environments at low speed has been introduced and tested. Moreover, a set of haptic feedback interfaces has been developed. Such devices are intended to evaluate any risky situation in order to make the bus driver aware of the danger of certain manoeuvres once pedestrians moving around the vehicle have been detected.

The effectiveness of the developed safety system has been analysed through some experiments carried out using a simulated scenario. These experiments show that, when a dangerous manoeuvre happens, the proposed system improves safety significantly. The number of medium and high risk situations as well as the number of collisions is clearly reduced, given that driver's time of reaction when braking is also lower and average time to collision increases with respect to situations where the system is disabled.

An ANOVA analysis has been performed to test the significance of the proposed safety systems. From the results obtained, we can conclude that there is a significant improvement on the time of reaction using the haptic throttle pedal, particularly when departing (accelerating). There is also a significant improvement on the time to collision as a consequence of the emergency brake, particularly when approaching to a bus stop (decelerating).

We have proved that there is no influence of the driver, which means that the safety system improves driving performance independently of driver's skills. In addition to this, the haptic steering wheel has also shown to be influential, particularly in turns, reducing the time of reaction even more when combined with the haptic throttle pedal.

Acknowledgements

This paper has been funded by Ministerio de Ciencia e Innovación (Spain) through the projects "Sistemas Avanzados de Seguridad Integral en Autobuses (SAFEBUS)" (IPT-2011-1165-370000) and "Sistemas de Conducción Segura de Vehículos de Transporte de Pasajeros y Materiales con Asistencia Háptica/Audiovisual e Interfaces Biomédicas (SAFETRANS)" (DPI2013-42302-R). This work was also supported by Programa VALi+d (Generalitat Valenciana). The authors wish to thank José Luís Sánchez Carrascosa for his dedication and commitment to the project and thanks to Ana Isabel Sánchez Galdón for her valuable help regarding ANOVA analysis.

References

[1] ERF, "European road statistics," European Union Road Federation, Tech. Rep., 2012.

[2] CARE Database, "Traffic safety basic facts: Heavy goods vehicles and buses," European Road Safety Observatory, Tech. Rep., 2015.

[3] ——, "Traffic safety basic facts: Pedestrians," European Road Safety Observatory, Tech. Rep., 2015.

[4] NHTSA's National Center for Statistics and Analysis, "School-transportation-related crashes," National Highway Traffic Safety Administration (USA), Tech. Rep., 2014.

[5] H. Schittenhelm, "Advanced brake assist – real world effectiveness of current implementations and next generation enlargements by mercedes-benz," in *23rd International Technical Conference on the Enhanced Safety of Vehicles (ESV)*, no. 13-0194, 2013.

[6] NHTSA's National Center for Statistics and Analysis, "Critical reasons for crashes investigated in the national motor vehicle crash causation survey," U.S. Department of Transportation, Tech. Rep., February 2015.

[7] R. Jurecki, M. Jaśkiewicz, M. Guzek, Z. Lozia, and P. Zdanowicz, "Driver's reaction time under emergency braking a car - research in a driving simulator," *Maintenance and Reliability*, vol. 14, no. 4, p. 295–301, 2012.

[8] X. Ma and I. Andréasson, "Driver reaction time estimation from the real car following data and its application in gm-type model evaluation," *Transportation Research Record*, 2006.

[9] T. Magister, R. Krulec, M. Batista, and L. Bogdanović, "The driver reaction time measurement experiences," in *Innovative Automotive Technology (IAT'05) conference*, 2005.

[10] D. Fambro, R. Koppa, D. Picha, and K. Fitzpatrick, "Driver perception-brake response in stopping sight distance situations," *Transportation Research Record, 1628: 1–7*, 1998.

[11] P. Stahl, B. Donmez, and G. Jamieson, "Anticipation in driving: The role of experience in the efficacy of pre-event conflict cues," *Human-Machine Systems, IEEE Transactions on*, vol. 44, no. 5, pp. 603–613, Oct 2014.

[12] N. Kaempchen and D. K., "Fusion of laserscanner and video for advanced driver assistance systems," in *11th World Congress on Intelligent Transportation Systems (ITS), Japan*, 2004, pp. 1–5.

[13] T. Gandhi and M. Trivedi, "Pedestrian collision avoidance systems: a survey of computer vision based recent studies," in *IEEE Intelligent Transportation Systems Conference*, 2006, pp. 976–981.

[14] D. Geronimo, A. Lopez, A. Sappa, and T. Graf, "Survey of pedestrian detection for advanced driver assistance systems," *Pattern Analysis and Machine Intelligence, IEEE Transactions on*, vol. 32, no. 7, pp. 1239–1258, July 2010.

[15] C. Wu, L. Peng, Z. Huang, M. Zhong, and D. Chu, "A method of vehicle motion prediction and collision risk assessment with a simulated vehicular cyber physical system," *Transportation Research Part C*, vol. 47, pp. 179–181, 2014.

[16] D. Brscic, T. Kanda, T. Ikeda, and T. Miyashita, "Person tracking in large public spaces using 3-d range sensors," *Human-Machine Systems, IEEE Transactions on*, vol. 43, no. 6, pp. 522–534, Nov 2013.

[17] J. H. Hogema, S. C. D. Vries, J. B. V. Erp, and R. J. Kiefer, "A tactile seat for direction coding in car driving: Field evaluation," *IEEE Transactions on Haptics*, vol. 2, no. 4, pp. 181–188, 2009.

[18] E. Adell, A. Varhelyi, M. Alonso, and J. Plaza, "Developing human-machine interaction components for a driver assistance system for safe speed and safe distance," *IET Intelligent Transport Systems*, vol. 2, no. 1, pp. 1–14, 2008.

[19] E. Adell, A. Várhelyi, and M. Hjälmdahl, "Auditory and haptic systems for in-car speed management - a comparative real life study," *Transportation Research Part F*, vol. 11, no. 1, pp. 445 – 458, 2008.

[20] M. Saffarian, J. de Winter, and R. Happee, "Enhancing driver car-following performance with a distance and acceleration display," *Human-Machine Systems, IEEE Transactions on*, vol. 43, no. 1, pp. 8–16, Jan 2013.

[21] S. M. Straughn, R. Gray, and H. Z. Tan, "To go or not to go: Stimulus-response compatibility for tactile and auditory pedestrian collision warnings," *IEEE Transactions on Haptics*, vol. 2, no. 2, pp. 111–117, 2009.

[22] F. Danieau, A. Lécuyer, P. Guillotel, J. Fleureau, N. Mollet, and M. Christie, "Enhancing audiovisual experience with haptic feedback: A survey on hav," *IEEE Transactions on Haptics*, 2013.

[23] F. Mars, M. Deroo, and J.-M. Hoc, "Analysis of human-machine cooperation when driving with different degrees of haptic shared control," *IEEE Transactions on Haptics*, vol. 7, no. 3, pp. 324–333, 2014.

[24] S. de Nijs, M. Mulder, and D. Abbink, "The value of haptic feedback in lane keeping," in *Systems, Man and Cybernetics (SMC), 2014 IEEE International Conference on*, Oct 2014, pp. 3599–3604.

[25] M. Mulder, D. Abbink, M. van Paassen, and M. Mulder, "Design of a haptic gas pedal for active car-following support," *Intelligent Transportation Systems, IEEE Transactions on*, vol. 12, no. 1, pp. 268–279, March 2011.

[26] S. M. Petermeijer, D. A. Abbink, M. Mulder, and J. C. F. de Winter, "The effect of haptic support systems on driver performance: A literature survey," *IEEE Transactions on Haptics*, 2015.

[27] L. Armesto, L. Arnal, J. Dols, V. Girbés, and J. C. Peris, "Safebus project: Advanced safety systems in buses," *RIAI (In press)*, pp. 1–12, 2015.

[28] B. Siciliano and O. Khatib, Eds., *Springer Handbook of Robotics*. Springer, 2008.

[29] P. Ioannou and Z. Xu, "Throttle and brake control systems for automatic vehicle following," *IVHS Journal*, vol. 1, no. 4, pp. 345–377, 1994.

[30] M. Hazewinkel, Ed., *Minkowski addition*. Springer, 2001, vol. Encyclopedia of Mathematics.

[31] U. Palmquist, "Intelligent cruise control and roadside information," *Micro, IEEE*, vol. 13, no. 1, pp. 20–28, 1993.

APPENDIX

A. Index of Multimedia Data

Table V. MULTIMEDIA FILES.

Item #	Type	File
1	Video	Multimedia_#1.avi
2	Video	Multimedia_#2.avi

Vicent Girbés received the B.Eng. (Hons) in Electronics and Control in 2009 and the M.Sc. in Control and Computer Science in 2010, both from the Universitat Politècnica de València (UPV), Spain. He was awarded 1st Best B.Eng. National Prize from the Spanish Ministry of Education, and also with an Academic Performance Award from the Valencian Government (GVA). In 2009 Mr. Girbés joined the Robotics and Automation Research Group of the Design and Manufacturing Institute (IDF-UPV). From 2010 to 2014 he held a former researcher fellowship in the VALi+d Program (GVA). During 2015 he has been working on two Spanish national projects: SAFEBUS and SAFETRANS. In 2013 he was visiting researcher at the Laboratory for Control of Uncertain Dynamical Systems of the University of Manchester (UK). He is currently working toward the Ph.D. degree in the field of smooth planning and control in intelligent vehicles, applied to autonomous and manual-assisted driving.

Leopoldo Armesto received the B.Sc. degree in Electronic Engineering, the M.Sc. degree in Control Systems Engineering, and the Ph.D. in Automation and Industrial Computer Science from the Universitat Politècnica de València (UPV), Spain, in 1998, 2001, and 2005, respectively. He held a Ph.D. Scholarship for three years at the Department of Systems Engineering and Control at the same University, where he is Assistant Professor since 2004. He is currently member of the Robotics and Automation Research Group of the Design and Manufacturing Institute (IDF-UPV). His current research interests are Mobile Robotics, Optimal Control, Advanced Driving Assistance Systems, 3D Printing and Reinforcement Learning. He is supervising 2 Ph.D. theses and has supervised 6 final M.Sc. Projects. He has participated in 20 Research Projects (leading 6 of them) and many other contracts with industry. He has published 8 JCR journal papers and 60 conference papers (google h-index 10).

Juan Dols is Industrial Engineer (Mechanics) since 1987 and in 1996 the Ph.D. degree at Technical University of Valencia-UPV (Spain), where he is now teaching Automotive and Transportation Engineering at the Mechanical and Materials Engineering Department of UPV. Professor Dols is also Director of the UPV Automobile Laboratory (LAUPV). His research activity is based in the design and development of driving simulators, wheelchair tiedown and occupant restraint systems, active and passive safety in vehicles, accessible transportation engineering, driving aids design and development, accident reconstruction technologies and vehicle dynamics. He has conducted as main researcher and coordinator several national projects (SEMAV, SATRUS, DGT, DATOS, ASUCAR, SE2RCO) and international EU funded projects (FORCE, ADAPT, TRAINER, CONSENSUS, IDEA, ASK-IT) in the 4th, 5th and 6th framework EU research programs. He also serves in the Editorial Board of the "Securitas Vialis" Journal, and has participated as reviewer in "Assistive Technology" and "Ergonomics" journals. Professor Dols has been Chairman of working group ISO TC22/WG4 "Accessibility in Public Transport Vehicles", and member of ISO TC173/SC1/WG6 "Restraint Systems for the Transport of Handicapped People in Wheelchairs", and full member of SAE, STA, EMG professional associations.

Josep Tornero received in 1982 the M.S. Degree in Systems and Control from the University of Manchester, Institute of Science and Technology and in 1985 the Ph.D. in Electrical Engineering at the Technical University of Valencia, Spain. He is currently Professor at the Department of Systems Engineering and Control, Head of the Robotics and Automation Research Group and also Director of the Design and Manufacture Institute of the Technical University of Valencia. He has been Visiting Professor at: the CIRSSE (NASA Center for Intelligent Robotics Systems for Space Exploration); the Rensselaer Polytechnic Institute at Troy (New York); and at the Department of Mechanical Engineering at the University of California (Berkeley). He is particularly interested in: modelling, control, and simulation of auto-guided-vehicles and robot arms; modelling, analysis, and control of multi-rate sampled data systems; as well as in collision detection/avoidance and automatic trajectory generation. Dr. Tornero has participated in many European research projects such as ESPRIT, BRITE, EUREKA and STRIDE, and in educational projects as ERAMUS, INTERCAMPUS, ALPHAS and TEMPUS.